Diplomarbeit

Clinicopathological characterization of osteoid osteomas treated in a single institution and comparison of two treatment modalities – a retrospective study

eingereicht von

Michael Meszarics

zur Erlangung des akademischen Grades

Doktor der gesamten Heilkunde

(Dr. med. univ.)

an der

Medizinischen Universität Graz

ausgeführt am

Institut für Pathologie

unter der Anleitung von

Univ. FÄ Priv.-Doz.in Dr.in med. univ. et scient. med. Iva Brcic

OÄ Dr.in Dr.in med. univ. Jasminka Igrec

Graz, am 18.03.2023

Eidesstattliche Erklärung

Ich erkläre ehrenwörtlich, dass ich die vorliegende Arbeit selbstständig und ohne fremde Hilfe verfasst habe, andere als die angegebenen Quellen nicht verwendet habe und die den benutzten Quellen wörtlich oder inhaltlich entnommenen Stellen als solche kenntlich gemacht habe.

Graz, am 18.03.2023 *Michael Meszarics eh*

Danksagung

Einen besonderen Dank möchte ich meinen zwei Betreuerinnen aussprechen, Univ. FÄ Priv.-Doz.in Dr.in med. univ. et scient. med. Iva Brcic und OÄ Dr.in Dr.in med. univ. Jasminka Igrec, die mir jederzeit beim Verfassen der Diplomarbeit zur Seite standen.

Ganz besonders möchte ich meinen Eltern danken, die mir stets den nötigen Rückhalt gaben, mich geduldig in all meinen Vorhaben und Entscheidungen unterstützten. Ohne euch wäre ich nicht zu diesem Menschen geworden, der ich heute bin. Dafür bin ich euch unendlich dankbar.

Zu guter Letzt möchte ich mich noch insbesondere bei meiner Freundin bedanken, die mich in der gesamten Studienzeit, stets motivierend und verständnisvoll begleitet hat. Vielen Dank für die unzähligen gemeinsamen Lernstunden, in denen wir Höhen und Tiefen gemeinsam meisterten. Danke, dass du so eine Bereicherung in meinem Leben bist.

Inhaltsverzeichnis - Table of Contents

Glossar und Abkürzungen – List of Abbreviations

COX ..... *cyclooxygenase*
CR ..... *conventional radiographs*
CT ..... computed tomography
ECM ..... *extracellular matrix*
FGF23 ..... *fibroblast growth factor 23*
M-CSF ..... macrophage colony stimulating factor
MRI ..... magnetic resonance imaging
MSC ..... *multipotent mesenchymal stem cell*
MVs ..... *matrix vesicles*
OO ..... osteoid osteoma
OPG ..... *osteoprotegerin*
PTH ..... Parathormone
RANK ..... *receptor activator of nuclear factor-κB*
RANKL ..... receptor activator of nuclear factor-κB ligand
RFA ..... *radiofrequency ablation*

Abbildungsverzeichnis - List of figures

Tabellenverzeichnis – List of tables

Zusammenfassung

Einleitung: Das Osteoidosteom (OO) ist ein gutartiger knochenproduzierender Tumor. Es ist radiologisch durch einen intrakortikalen Nidus mit unterschiedlich starker Verkalkung und kortikaler Verdickung, Sklerose und Knochenmarködem gekennzeichnet. Der Nidus hat ein selbstlimitierendes Wachstum, ist normalerweise asymptomatisch und heilt spontan aus. Das typische klinische Erscheinungsbild des OO besteht aus nächtlichen Schmerzen, die durch die Verabreichung von Salicylaten sofort gelindert werden können. OO können mittels Computertomographie (CT) und der Magnetresonanztomographie (MRT) je nach ihrer Lokalisation im Knochen wie folgt eingeteilt werden: subperiostal, intrakortikal, endostal und medullär. Die CT-geführte perkutane Radiofrequenz Ablation (RFA) ist eine einfache, minimal-invasive, sichere und hochwirksame Technik zur Behandlung von OO. Offene Operationen sollten Fällen mit diagnostischer Unsicherheit oder Wirbelsäulenläsionen vorbehalten bleiben, die auf eine medizinische Behandlung nicht ansprechen und/oder aufgrund der anatomisch engen Beziehung zu lebenswichtigen Weichteilstrukturen nicht sicher erhitzt werden können. Das Ziel dieser Studie war es, epidemiologische, klinische und radiologische Befunde zusammenzufassen und die Behandlungsergebnisse von Patienten:innen mit OO zu bewerten, die in unserer Einrichtung behandelt wurden.

Methoden: Von Januar 2005 bis September 2019 wurden 122 Patienten:innen mit OO retrospektiv untersucht. Die Patienten:innen wurden aus einer prospektiv gepflegten Tumordatenbank unter Verwendung von histologischen (für Patienten:innen, die sich einer Operation unterziehen) oder radiologischen diagnostizierten OO ausgewählt. Die Studie umfasste 43 (35 %) Frauen und 79 (65 %) Männer; das mittlere Alter der Patienten:innen betrug 21,2 Jahre. Durchgeführte Bildgebungen wurden auf das Vorhandensein typischer Merkmale eines OO analysiert.

Ergebnisse: Die OO waren am häufigsten im Femur (n=39; 32 %), der Tibia (n=37; 30,3 %), dem Humerus (n=9; 7,4 %) und dem Radius (n = 4; 3,3 %) lokalisiert. Der Rest (n=34, 27,9%) befand sich in Wadenbein, Wirbelsäule, Füßen, Kreuzbein, Händen, Schulterblatt, Kniescheibe, Elle und Hüftgelenkspfanne. Die Läsionen waren in 79,5 % der Fälle kortikal gelegen. Bei einem Patienten waren die Läsionen multifokal. CTs wurden bei 108

Patienten:innen und MRTs bei 106 Patienten:innen durchgeführt. Der mittlere Durchmesser des Nidus betrug um die 8,65 ± 5,0 mm (Bereich 2–25 mm). Die Verzögerung der Diagnosestellung betrug 13,3±17,4 Monate. Insgesamt wurden 118 Patienten:innen in unserer Einrichtung behandelt: davon 71 (60,2 %) mittels RFA und 42 (35,6 %) mittels Operation. 5 (4,2 %) Patienten:innen wurden mit beiden Methoden behandelt, 4 Patienten:innen erhielten nur eine konservative Therapie. Bei allen Operationsproben (n=42) wurde die Diagnose OO pathohistologisch bestätigt. Die primäre klinische Erfolgsrate für die Behandlung mittels RFA betrug 90,1 % und die der chirurgisch behandelten Patienten:innen 81,0 %. Der sekundäre klinische Erfolg betrug in beiden Gruppen 100 %. Bei den meisten Patienten:innen wurde nach einem Tumorrezidiv die gleiche Art von Verfahren durchgeführt. Bei zwei Patienten wurde zunächst eine RFA-Behandlung durchgeführt, gefolgt von einer chirurgischen Exzision nach dem erneuten Auftreten klinischer Symptome und einem radiologisch bestätigten Tumorrezidiv. 9,9 % der mit RFA behandelten Patienten:innen entwickelten Komplikationen.

Schlussfolgerung: OO findet sich überwiegend bei männlichen Patienten, tritt häufig in den unteren Extremitäten auf und ist meist kortikal lokalisiert. In Übereinstimmung mit der Literatur wurde eine signifikante Verzögerung bei der Diagnose von OO beobachtet. Die RFA ist im Vergleich zur chirurgischen Behandlung eine zuverlässige und effiziente Behandlungsoption bei OO.

Abstract

Introduction: Osteoid osteoma (OO) is a benign bone-producing tumor. Radiologically, it is characterized by an intracortical nidus, with calcification and cortical thickening, sclerosis, and bone marrow edema. The nidus has self-limiting growth, with time it becomes asymptomatic and heals spontaneously. The characteristical clinical presentation is the night pain that relieved by salicylates. On computed tomography (CT) and magnetic resonance imaging (MRI) findings, OO can be classified according to their location as: medullary, endosteal, intracortical and subperiosteal. CT-guided percutaneous radiofrequent ablation (RFA) is a safe, minimally invasive, technique for treatment of OOs. Surgical resection/curettage is reserved for spinal lesions or unclear cases. The aim of our study was to summarize epidemiological, clinical, and radiological data of patients with OOs treated in our institution. In addition, we wanted to evaluate the treatment results.

Methods: We retrospectively studied 122 patients with OO in the period from January 2005 to September 2019. Patients were selected from a tumor database using either histological (for those patients undergoing surgery) or radiological diagnosis of OO. Available imaging examinations performed were analyzed for the presence of typical imaging findings of OO.

Results: The study included 43 (35%) females and 79 (65%) males; mean patient age was 21.2 years. The OOs were most frequently located in the femur (n=39; 32%), the tibia (n=37; 30,3%), the humerus (n=9; 7,4%), and the radius (n=4; 3,3%). The rest (n=34, 27,9%) were found in sacrum, spine, scapula, feet, hands, ulna, fibula, patella, and acetabulum. Lesions arose cortically in 79.5% of patients. In one case, the tumors were multifocal. CT was performed in 108 and MRI in 106 patients. The mean nidus size was 8.65±5,0 mm (range 2 –25 mm). The tumors were diagnosed with a delay of 13.3±17.4 months. Finally, a total of 118 patients were treated in our institution: 71 (60.2%) were treated with RFA and 42 (35.6%) underwent surgery. 5(4.2%) patients underwent both treatments. Last four patients received only conservative treatment. The primary clinical success rate was 90,1%, and 81,0% for RFA and surgery, respectively, while the secondary clinical success was 100% in both groups. In 9,9% of the patients undergoing RFA complications developed.

Conclusion: OO is more frequently arising in male patients, is usually found in the lower extremities, and is most commonly located cortically. The delay in the diagnosis is significant in patients with OO – this could be prevented by good clinical history and proper radiological methods. When compared to surgical treatment, RFA is a safe, reliable and efficient method for OO treatment.

1 Introduction

1.1 Anatomic and physiologic basis of bones

The human musculoskeletal system is composed of two components: 1) the main active component (muscles) and 2) passive component including bones, cartilages, joints and their attending ligaments, and all components of the musculoskeletal system are highly specialized body tissues. The adult human skeleton is made up of 206 bones, although the exact number of small bones can vary individually (1).

The functional interaction of active and passive elements enables the body to perform three main physiological functions: movement, protection, and metabolic activity. The mechanical nature of bone gives support for movement and physical stability, as well as protection by encasing vulnerable inner organs. The bone is a reservoir for many ions, especially calcium and phosphate. In addition, the innermost part of the bone, the medullary cavity or medulla, forms an environment for bone marrow and fat, and is involved in the progression of hematopoietic stem cells (2).

Living bone is a very reactive and dynamic tissue that can reply to various metabolic, physical, and endocrine stimuli. It also has the ability to re-establish its normal function and architecture after injury/trauma (3).

1.1.1 Topographic characteristic

The most important topographical regions of the skeleton are visualized in Figure 1. The skeleton can be divided in three different parts: 1) the axial skeleton formed of bones along the body's central axis like the skull, vertebral column and sacrum; 2) the appendicular skeleton built of bones of the extremities, the scapula and pelvis; and 3) the acral skeleton including the small bones of the hands and feet (3).

In general, bones can be classified into two basic groups of flat and tubular ones. The skull, mandible, scapulae, sternum, and ribs belong to flat bones. Bones of the extremities are tubular, which can be categorized into long and short bones. Long bones include the humeri, radii, ulnae, metacarpals, femurs, tibiae, fibulae, metatarsals, phalanges, and clavicles. Short bones include the carpal and tarsal bones, patellae, and sesamoid bones. The vertebrae, sacrum, coccyx, and hyoid bone are called irregular bones because they differ in their basic form.

Flat and long bones are developed differently, flat ones are made up of membranous bone formation and long tubular bones are made up of a combination of membranous and endochondral bone formation (4).

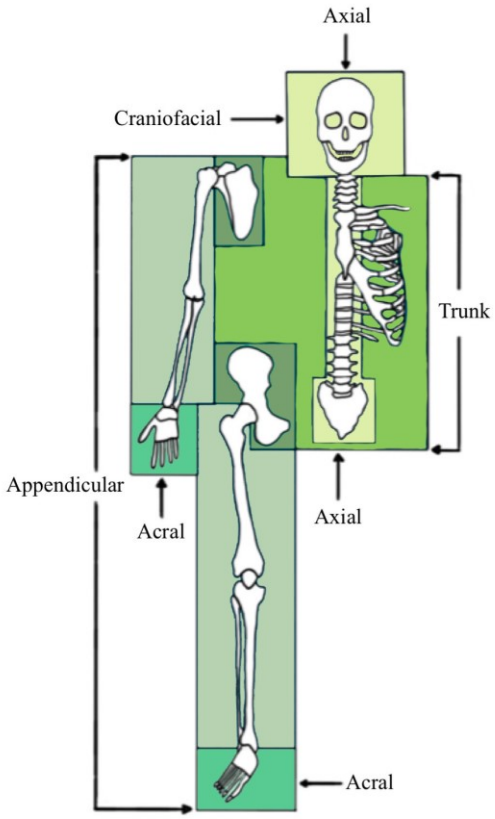

Figure 1: Topographical classification of skeleton showing most important topographical regions. (Reference: From Dorfman and Czerniak's Bone Tumors p. 4.)

Tubular bones are made up of different zones (Fig. 2). The proximal and distal end zone of bones is called epiphysis, is located between the growth plate and the end of the bone and is covered with cartilage. The rounded epiphysis forms a joint with other connected bones.
The region adjacent to it is called metaphysis and is composed of a layer of hyaline cartilage, also known as epiphyseal plate which is relevant for the length growth of the hollow shaft. As the bone grows, the hyaline cartilage of the epiphyseal plate gets replaced by bone and the remaining line is called the epiphyseal line. The metaphysis and epiphysis are built of trabecular bone, surrounded by the substantia compacta which is a compact layer of lamellar bone. Finally, the area between the proximal and distal end of bone is called diaphysis. It is a long, cylindrical shaft, built of tight cortical bone which surrounds the bone marrow in the inner medullar cavity.

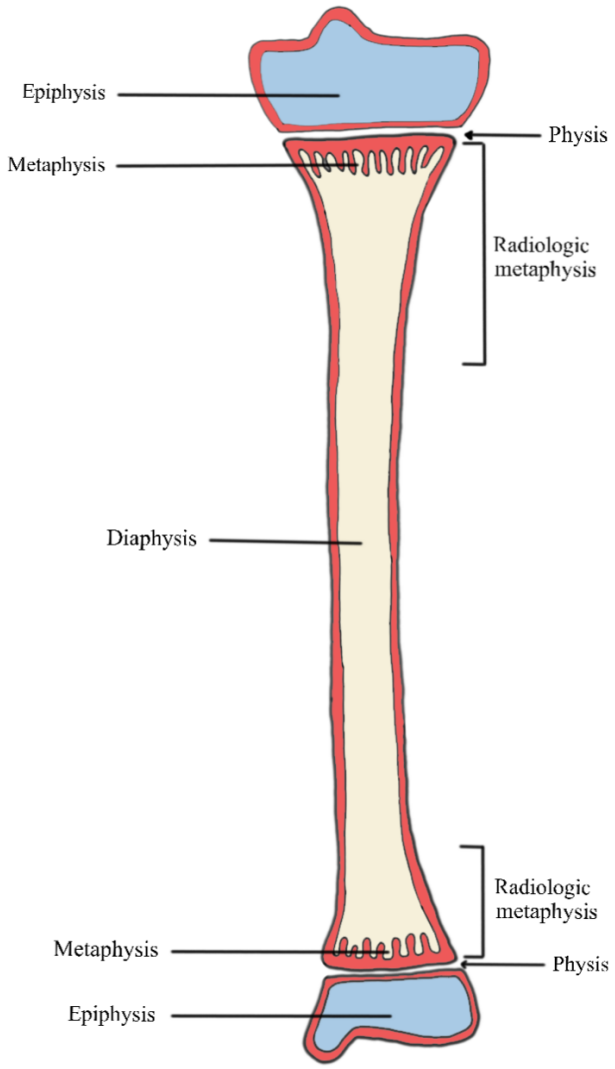

Figure 2: Topographical zones of tubular bone. (Reference: From Dorfman and Czerniak's Bone Tumors p. 5)

1.1.2 Bone

The adult skeleton can be divided into two major bone types, depending on the skeletal sites and type of bone. The inner bone substance (spongiosa) and the proximal and distal ends of long bones are built of a honeycomb-like network of trabeculae. It is also known as spongy

bone because of its honeycomb-like architecture, made up of trabecular plates and rods (4). The lamellae in the spongiosa are parallel disposed to the trabecular surface (5) and are embedded in a good vascularized bone marrow that occupies near 80% of the volume (6). (In comparison to cortical bone, trabecular one is metabolically more active and serves as mineral supplier in deficiency states.) In comparison to cortical bone, trabecular one has a larger surface/ volume ratio (3), exposed to the bone marrow and blood flow, thus the bone turnover is higher (7) and more sensitive for variation in the mineral homeostasis (8).

On the other hand, the dense and compact cortical bone is relevant for mechanical strength and protection. About 80% of the volume in cortical bone is mineralized (9). The construction of compact bone is based on a network of osteons. One osteon contains a central haversian canal, and lamellae are tightly packed in concentric circles around it. The vascular supply of the bone substance and neural tissue is ensured by blood vessels located in the Haversian canals. These blood vessels sprout radial into Volkmann canals, a cross-connections in the cortex (5, 6).

In general, the outer cortical surface of bone is surrounded by a dense fibrous connective tissue sheath, called the periosteum. It is composed of two different layers, the outer stratum fibrosum and the inner stratum osteogenicum. The stratum fibrosum is built of thick collagenous fibers, also called Sharpey's fibers. The stratum osteogenicum, which is directly adjacent to the cortical bone, contains numerous blood and lymphatic vessels, nerves, and inactive bone specific cells, like osteoclasts and osteoblasts. Accordingly, the main functions of the periosteum are nutrition of the adjacent bone, healing of the bone after injuries and the radial growth (5, 10).

The surface of the inner cavity of the bone is covered by an endosteal lining consisting of a one layer of flat bone lining cells that lie on a thin layer of collagenous and reticular fibers. Similar to the periosteum, osteoclasts and osteoblasts are also found in the endosteum and have an important function on remodeling and healing of cortical and trabecular bone (11).

Bone marrow is located inside the central cavities of long and axial bones. Its basic framework is built of reticular tissue, which contains hematopoietic stem, progenitor, and fat cells. The red colored bone marrow receives its typical color due to a process called hematopoiesis, in which blood cells, especially erythrocytes, are formed.

As a newborn child, the relative amount of active red bone marrow in bones is much higher than in adult ones. As one gets older, the active hematopoietic bone marrow is transformed to fatty bone marrow, also known as inactive hematopoietic yellow marrow substance. Healthy adults maintain the active red marrow in proximal endings of humerus and femur, as well as in the axial skeleton bones like sternum, vertebrae, ribs, scapula and pelvic bones (5).

The bone marrow in long bones is supplied via nutrient canals, which comprises of a nutrient artery and one or two nutrient veins passing through the cortical bone into the bone marrow cavity. The marrow of flat bones is vascularized by blood vessels coming from the large and small nutrient canals (11).

1.1.3 Extracellular matrix

The three main components of the extracellular matrix (ECM) of bones are collagen fibrils, hydroxyapatite, and proteoglycans.

The ECM of bones is made up of 90% organic collagenous proteins. Collagen functions as a scaffold on which calcium and phosphate are deposited in the form of inorganic hydroxyapatite. This gives the bone tissue its distinctive flexible and inflexible characteristics (6)

The organic amount of the bone matrix is basically type I collagen, with a small component of types III and V. Collagen is a right-handed triple helix compound of three helical peptide chains, also called alpha chains (5) and provides the ECM its strength and resilience (3).

In addition, the ECM is also composed of non-collagen organic components, like proteoglycans and glycoproteins which are particularly important for the strengthening of the collagen- scaffold and regulation of mineralization.

1.1.3.1 Bone matrix mineralization

The inorganic bone substance is principally made up of calcium and phosphate ions, which are bound together to form the hydroxyapatite crystals. Hydroxyapatite [Ca10 (PO4)6 (OH)2] is the major mineral element of bone, and it also contains small amounts of carbonate, magnesium and acid phosphatase (4). Bone is composed of 50 - 70% mineral, 20 - 40% organic matrix, 10% water, and <3% lipids (6).

1.1.4 Bone cells

Bone is composed of various specific cell types including osteocytes, osteoblasts, bone lining cells and osteoclasts (12). These cells, as well as progenitor cells for bone marrow stromal cells, chondrocytes, muscle cells, and adipocytes, develop from the multipotent mesenchymal stem cell (MSC) (Fig 3). Osteocytes are terminally differentiated osteoblasts comprising about 95% of all bone cells in an adult skeleton (5). These cells permeate the inner bone tissue and are surrounded by the mineralized bone matrix. Osteoblasts, bone lining cells and osteoclasts can be found on free bone surfaces (12).

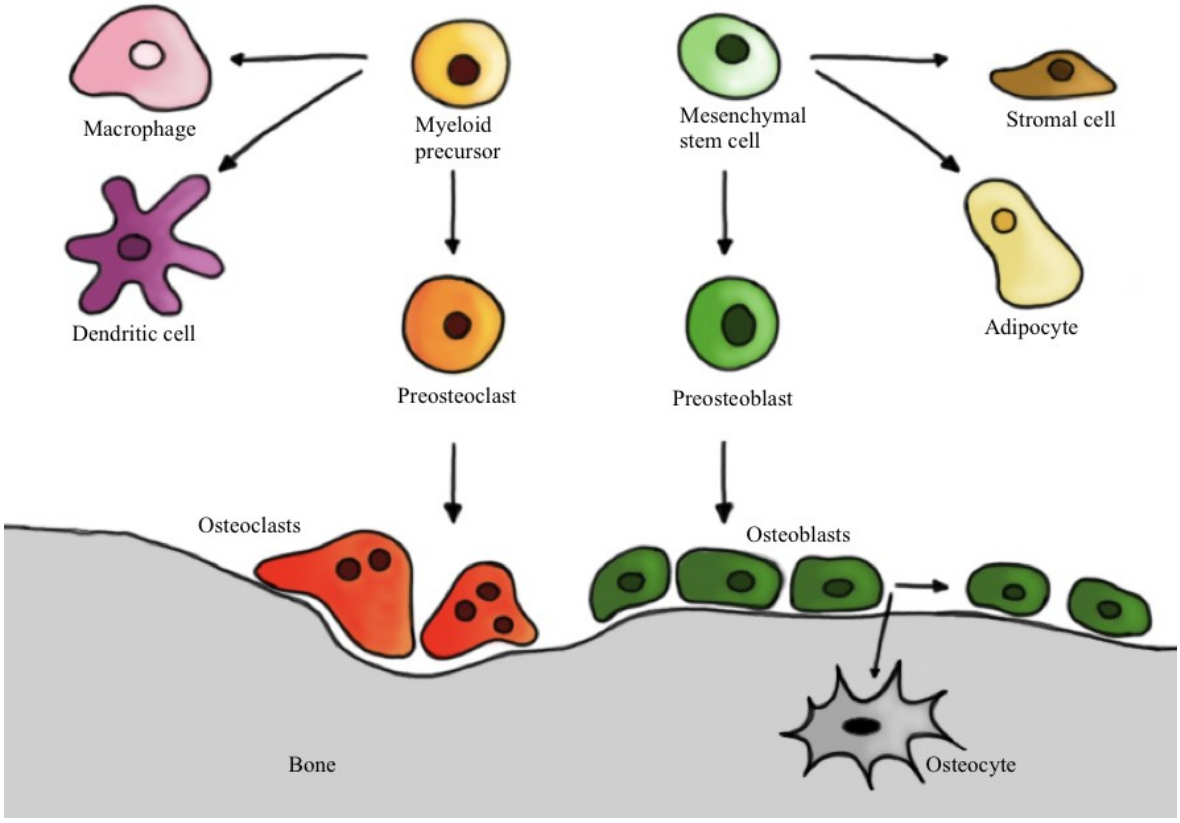

Figure 3: Graphic of bone cell differentiation. (Reference: From Osteoimmunology: Interplay Between the Immune System and Bone Metabolism, Walsh MC et al.)

1.1.4.1 Osteocytes

Osteocytes are long living special cells and represent the final stage of osteoblasts. They are located within lacunae in the inner bone tissue and are surrounded by the bone matrix and have radial outgoing fine canals called canaliculi.

They form a labyrinth of canals through the mineralized bone matrix, provide the main part of the bone cell syncytium, and enable the diffusion of substances across the bone. Osteocytes are connected by their long processes, which are extended from the central cell body into the canaliculi in the bone matrix, to other neighboring osteocytes-, osteoblasts-

and bone-lining-cells- processes by gap junctions (12). These intercellular connected channels permit direct cell to cell communication, maturation, and activity. Osteocytes secrete several important substances, which are essential for the bone remodelling and formation. They act as mechanoreceptors to detect physical stimuli in bone and are able to synthesize substances like sclerostin, which is important for the inhibition of bone formation or fibroblast growth factor 23 (FGF23) a protein, which increases the nephrotic excretion of phosphate (5). Additionally, osteocytes can express receptor activator of nuclear factor-κB ligand (RANKL), a membrane-bound ligand for receptor activator of nuclear factor-κB (RANK) required for the differentiation and function of osteoclasts (13).

1.1.4.2 Osteoblasts

Osteoblasts are cuboidal formed cells with big and prominent Golgi apparatus, rough endoplasmic reticulum and several secretory vesicles (14). Active osteoblasts can be found on bone-forming surfaces of bones, where they are synthesizing new bone matrix. They produce components of the bone matrix such as structural macromolecules, like type I collagen, certain proteoglycans and non-collagenous proteins. (12).

Moreover, osteoblasts are responsible for the mineralization of the non-mineralized organic part of bone matrix, also known as osteoid (5). The mineralization occurs due to released matrix vesicles (MVs) from mature osteoblasts. The MVs contain alkaline phosphatase and various enzymes (12) and form hydroxyapatite crystals from the enzymatical accumulation of calcium and phosphate ions. These crystals rupture the matrix vesicles to get into the ECM, where they grow further to finally attach to collagen fibrils and the ECM gets mineralized (5).
Like osteocytes, osteoblasts are also connected with each other by the gap-junctions and some of them are connected to osteocytes (15). At the end of their development, osteoblasts undergo either apoptosis or transform to osteocytes or bone lining cells (16). Bone lining cells are flat and fusiform cells and are located on the endosteum of trabecular and endosteal

bone surfaces facing the inner cavity. On the cortically mineralized bone surface the bone lining cells are located under the periosteum layer. The bone lining cells do not exist in bone regions where bone resorption or bone formation takes place.

Osteoblasts play a vital role in regulation of osteoclasts by the osteoprotegerin (OPG)/RANKL/RANK pathway. Thus, they can intervene in osteoclast formation, differentiation grade, activation, or apoptosis (17). Osteoblasts produce RANKL, which raises the quantity and activeness of osteoclasts, by linking on the osteoclastic receptor RANK.

The osteoclastogenesis is increased when RANKL binds to RANK on osteoclast progenitors. This process can be systematically inhibited by OPG, which is also excreted by osteoblasts and acts as a decoy-receptor for RANKL. OPG ties to RANKL and blocks the interaction of RANK and RANKL. As a result, the differentiation and activation of osteoclasts is stopped.

1.1.4.3 Osteoclasts

Osteoclasts are tall multinucleated cells, which descend from mononuclear cells of the hematopoietic stem cell lineage (5) and area member of the monocyte and macrophage family (18).

They migrate from the bone marrow through the surrounding cortical bone to the bone surface. Active osteoclasts attach directly to mineralized bone matrix and start the bone resorption (12). A key role for the formation and activation of osteoclasts is the cytokine, called macrophage colony stimulating factor (M-CSF). M-CSF is a membrane-bound protein secreted by osteoblasts, their precursors and osteocytes (19) (5). It promotes the proliferation and survival of osteoclasts precursors (19). In case that osteoclasts are currently needed on bone surfaces, M-CSF gets secreted and stimulates the expression of RANK on osteoclast progenitors (5) that needs to bind to its appropriate ligand located on osteoblast and osteocyte surfaces. The RANK/RANKL interaction pathway is essential for the osteocytic degeneration of bone matrix. Therefore, the stimulation of osteoclastogenesis depends on the right balance of M-CSF, RANK, RANKL and OPG (6). As the osteoclasts

bind on the bone matrix, they are polarized (4) and they form a region of tight contact between the cell and the surface. This point of contact is called sealing zone and is stabilized by a circle of actin filament (2, 5).

A distinctive feature of polarized osteoclasts is its "ruffled border". It is a sinuous cell membrane that is opposite to the bone surface and is influenced by peptide hormones (3)S.10. Parathormone (PTH) and calcitonin are responsible for the formation and adhesion of the ruffled membrane to the adjacent bone surface. PTH has a stimulating function and calcitonin an inhibiting one.

The ruffled membrane is the resorptive part of osteocytes (18). It excretes organic acids to dissolve the inorganic mineral components of the bone substance by low pH (12). Lysosomal enzymes, like Cathepsin K, serve to eliminate the organic bone matrix. The extracellular digested bone matrix is endocytosed by the osteocyte and transcytosed in vesicles through the cell body (5). Finally, it is secreted on the cell backside. The required energy for the secretion of lysosomal enzymes and resorption of bone minerals are provided by the vacuolar H+ -ATPases pump. This pump is located on the basolateral membrane of osteocytes (6).

Osteoclasts play an important role in the long-retention of blood calcium homeostasis (12). Disorders in osteoclast formation and activity might lead to bone diseases. Decreased activity causes enhanced bone mass, called osteopetrosis and on the other side increased osteoclastic activity causes decimated bone mass, known as osteoporosis (6, 18).

1.2 Bone tumors

Tumors of the human skeleton can be divided into primary and secondary bone tumors. Primary bone tumors show a wide spectrum of morphology and range in biological behavior from benign to highly malignant neoplasms. They are classified according to their tissue of origin (20). Skeletal metastases are secondary bone tumors that are 2,5- times more common than primary ones (21).

Primary bone tumors are rare, and for their accurate classification, correlation of clinical, radiological, and pathologic findings is needed. Reflecting the biological potential, bone

tumors can be categorized into four categories: benign, intermediate (locally aggressive), intermediate (rarely metastasizing) and malignant. These stages are defined in the fifth edition of the WHO Classification of Tumors series (22).

Benign: Benign bone tumors have a limited potential to recur locally. If a recurrence occurs, it is not destroying a surrounding structure and is always cured by complete local excision or curettage. These tumors do not metastasize.

Intermediate (locally aggressive): These bone tumors often recur locally and can grow in an infiltrative and locally destructive fashion. They do not have the potential to metastasize, however require wide excision with a free margin or local adjuvant irradiation to prevent recurrences.

Intermediate (rarely metastasizing): Bone tumors in this category grow locally with an aggressive pattern and can rarely metastasize (usually to the lung).

Malignant: Bone sarcomas grow locally in a destructive fashion, recur, and have a risk of developing distant metastasis.

Primary benign bone tumors are about 3- 4 times more common than malignant ones (21). Of note, as most benign bone tumors are asymptomatic and are usually incidentally discovered, the exact incidence is not known. Primary malignant bone neoplasms are uncommon and comprise 0.5% of all malignant tumors in the human body. They most commonly affect children and teenagers (21) and represent a significant cause of morbidity and mortality in this age group. The 2020 WHO classification of bone tumors is summarized in Table 1.

Table 1: WHO classification of bone tumors

Chondrogenic tumors

Benign
- Subungual exostosis
- Bizarre paraosteal osteochondromatouse proliferation
- Periosteal chondroma
- Enchondroma
- Chondroblastoma NOS
- Chondromyxoid fibroma
- Osteochondromyxoma

Intermediate (locally aggressive)
- Chondromatosis NOS
- Atypical cartilaginous tumor

Malignant
- Chondrosarcoma, grade 1
- Chondrosarcoma, grade 2
- Chondrosarcoma, grade 3
- Periosteal chondrosarcoma
- Clear cell chondrosarcoma
- Mesenchymal chondrosarcoma
- Dedifferentiated chondrosarcoma

Osteogenic tumors

Benign
- Osteoma NOS
- Osteoid osteoma NOS

Intermediate (locally aggressive)
- Osteoblastoma NOS

Malignant
- Low-grade central osteosarcoma
- Osteosarcoma NOS
  - Conventional osteosarcoma
  - Telangiectatic osteosarcoma
  - Small cell osteosarcoma
- Parosteal osteosarcoma
- Periosteal osteosarcoma
- High-grade surface osteosarcoma

Secondary osteosarcoma

Fibrogenic tumor

Intermediate (locally aggressive)
Desmoplastic fibroma

Malignant
Fibrosarcoma NOS

Vascular tumors of bone

Benign
Haemangioma NOS

Intermediate (locally aggressive)
Epitheloid haemangioma

Malignant
Epitheloid haemangioendothelioma NOS
Angiosarcoma

Osteoclastic giant cell-rich tumors

Benign
Aneurysmal bone cyst
Non-ossifying fibroma

Intermediate (locally aggressive, rarely metastasizing)
Giant cell tumor of bone NOS

Malignant
Giant cell tumor of bone, malignant

Notochordal tumors

Benign
Benign notochordal tumor

Malignant
Chordoma NOS
Chondroid chordoma
Poorly differentiated chordoma
Dedifferentiated chordoma

Other mesenchymal tumors of bone

Benign

Chondromesenchymal hamartoma of chest wall
Simple bone cyst
Fibrous dysplasia
Osteofibrous dysplasia
Lipoma NOS
Hibernoma

Intermediate (locally aggressive)

Osteofibrous dysplasia-like adamantinoma
Mesenchymoma NOS

Malignant

Adamantinoma of long bones
Dedifferentiated adamantinoma
Leiomyosarcoma NOS
Pleomorphic sarcoma, undifferentiated
Bone metastases

Hematopoietic neoplasms of bone

Plasmacytoma of bone
Malignant lymphoma, non-Hodgkin, NOS
Hodgkin disease NOS
Diffuse large B-cell lymphoma NOS
Follicular lymphoma NOS
Marginal zone B- cell lymphoma NOS
T- cell lymphoma NOS
Anaplastic large cell lymphoma NOS
Malignant lymphoma, lymphoblastic, NOS
Burkitt lymphoma NOS
Langerhans cell histiocytosis
Langerhans cell histiocytosis, disseminated
Erdheim- Chester disease
Rosai-Dorfman disease

1.2.1 Osteogenic tumors

Osteogenic tumors arise from neoplastic cells which differentiate along the osteoblastic line of development. Bone forming tumors are heterogeneous and have a wide range of morphology, biological potential, and behavior (Figure 4). Osteogenic tumors can be benign, locally inactive (osteoma, osteoid osteoma) or locally aggressive (osteoblastoma), or malignant (osteosarcoma) with aggressive and destructive growth. Detailed classification is shown in Table 1.

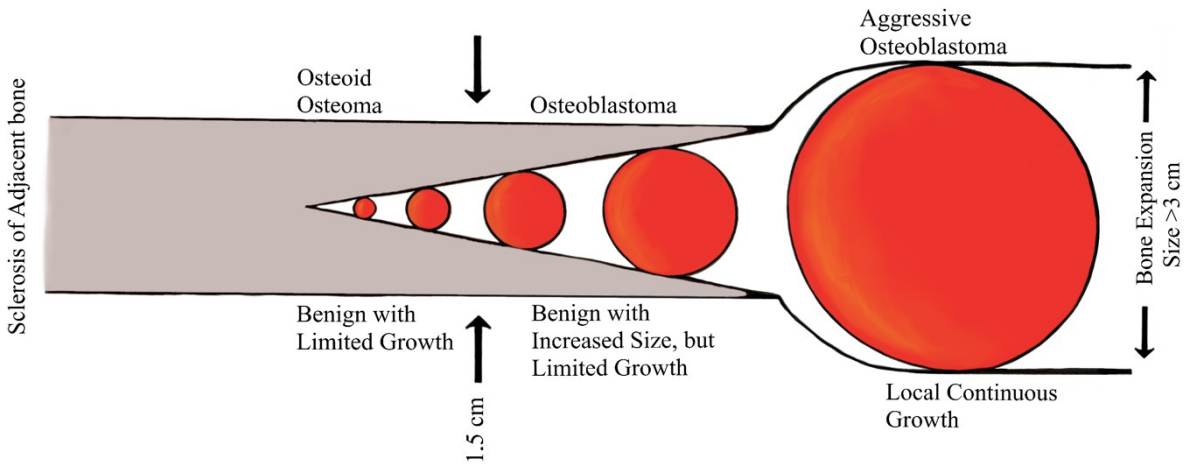

Figure 4: Comparison of biologic behaviour and growth potential of osteoblastic tumors (Reference: From Dorfman and Czerniak's Bone Tumors p. 144)

1.2.1.1 Osteoma

An osteoma is a slow- growing benign osteoblastic tumor. It is mainly composed of mature lamellar bone and affects primarily bone that is formed by membranous ossification, like in the calvarial, facial and jaw- bone (22) Osteoma arises at the bone surface and in the epiphysis and metaphysis of long bones and can be found as a singular or multiple lesions.

The latter is associated with Gardner syndrome. Furthermore, they can rarely be found in the pelvic bones and vertebra.
Both men and women are affected equally, the highest incidence is between the fourth to fifth decade of life. Osteomas are asymptomatic but in the head region they can cause headache, sinusitis, and nasal discharge up to loss of smell.

1.3 Osteoid Osteoma

Osteoid osteoma (OO) is a benign bone-forming tumor with a limited growth potential (23). Typically, it is up to 2 cm large lesion composed of nidus of osteoid tissue that has central areas of mineralization. This nidus is surrounded by a zone of reactive bone formation (23).

1.3.1 Epidemiology

OOs represent almost 3% of all primary bone tumors and is the third most common benign bone tumor (24). They represent about 10% to 12% of all benign bone tumors. Men are two times more commonly affected and the peak incidence is in the first two decades (11) (3) (6).

The long bones like the femur and tibia are most affected, followed by the small bones of the hands or feet (Fig. 5). Sometimes the lumbar part the spine can be affected (3). The osteoid osteoma mostly involves the cortex, less frequently cancellous or subperiosteal bone (22).

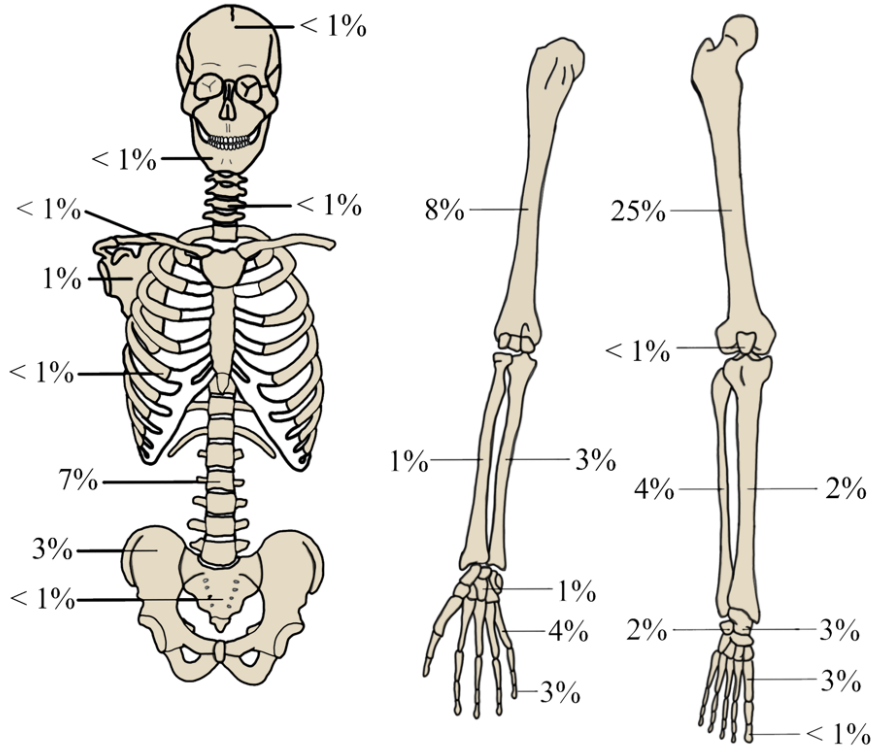

Figure 5: Skeletal distribution of osteoid osteoma (Reference: From Vincent J. Vigorita Orthopaedic pathology p. 342)

1.3.2 Clinics

The usual symptom is pain that can often get worse during the night (so called nocturnal pain) and can be alleviated by nonsteroidal anti- inflammatory drugs (NSAIDs), like aspirin (Zhang and Rosenberg, 2017). Pain gets triggered by afferent and unmyelinated nerve endings in the middle of the nidus (25). Immunohistochemical studies describe a high prostaglandin concentration in the nidus (26). Based on their vasodilatory and angiogenic characteristics, an intraosseous increase in pressure leads to irritation of the afferent nerve endings and causes pain.

Swelling is the second most common symptom due to the prostaglandin release within the nidus that causes an increased vascularization of tumor and adjacent soft tissue (27). In case of intraarticular or periarticular location of this benign tumor, the patient presents with joint pain, effusion, redness and local swelling, thus mimicking an inflammatory process (3).

Patients with lesion located in the vertebrae often have a painful reactive scoliosis caused by an unilateral spasm of the paravertebral muscles (28). Others may have constrained movement in the spine and localized tenderness. Therefore, radiologic imaging plays a significant role in a diagnostic workup.

1.3.3 Radiology

Radiologically the OO is ovaloid lesion, with a central radiolucent nidus, less than 1.5 or 2 cm in diameter, with various amounts of mineralization, surrounded by a distinct zone of dense sclerosis and periosteal bone formation (23).

The computed tomography (CT) is imaging method of choice in the evaluation of patients with OO. The highest diagnostic accuracy is achieved by obtaining the high-resolution CT images with slice thickness of 1-2 mm and bone window setting. (29). Although magnetic resonance imaging MRI is sensitive for the depiction of bone and soft-tissue edema, osteitis and synovitis, it is non-specific and is often unable to identify the nidus (30).

Depending on the localization, for instance lesion located in the long bone vs. intraarticular vs. lesion in the axial skeleton, the imaging characteristics of the OO differ, and range from mild sclerosis of the cancellous bone to extensive periosteal reaction with new bone formation (3).

There are also certain radiographic features of OO depending on site of origin, cortical, medullary and subperiosteal. OO is often found in the cortical layer with its typical characteristics. The detection of the nidus in the medullary type of OO can be very difficult, due to formation of osteosclerosis at a distant point(31). This prevents peripheral reactive bone formation. Without reactive bone formation, detection of the nidus gets complicated.

A radionuclide bone scan can simplify the detection (32).

OO located subperiosteally (adjacent to the outer margin of the native cortex) show cortical thickening and adjacent reactive sclerosis in a long bone shaft, which may, on conventional radiographs (CR) and CT, obscure the nidus (29). Clinical presentation of the intraarticular osteoid osteomas is often nonspecific and imaging findings on MRI, including periosteal

rection, bone- and soft tissue edema, and synovial hypertrophy, can mimic other neoplastic, inflammatory and posttraumatic changes (stress fracture, septic or chronic inflammatory arthritis , osteomyelitis or a bone malignancy, such as Ewing sarcoma) (33). Often nidus can be masked by extensive bone marrow edema. In this case, the skeletal scintigraphy is a valuable imaging tool (34).

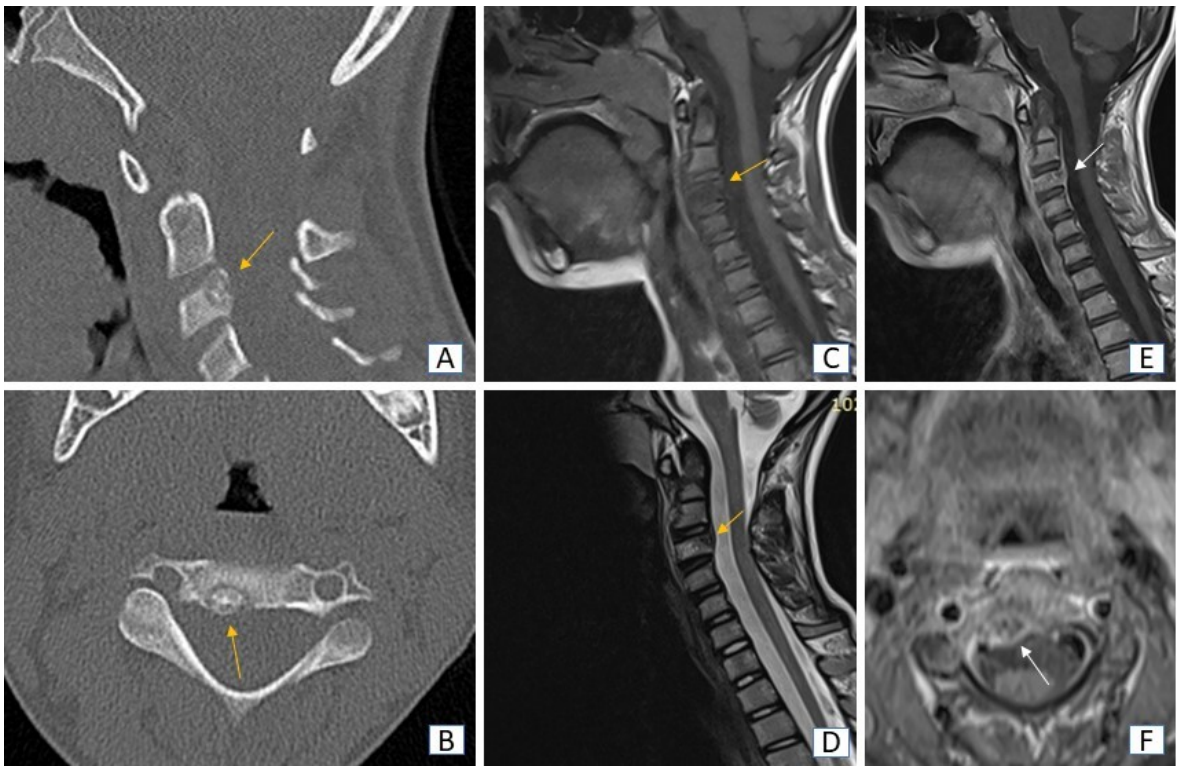

Figure 6: Osteoid osteoma of the third cervical vertebra in 5-year-old female patient. Sagittal (A) and axial (B) high resolution CT images of the osteoid osteoma with affection of the posterior lamina (white arrow). Sagittal T1-weighted (C) and T2-weighted (D) MRI images show heterogenous signal of the tumor, due to calcification (white arrow), and surrounding bone-marrow edema in T2-weighted sequence. On sagittal (E) and axial (F) post-contrast MRI images there is heterogenous contrast enhancement of the lesion.

1.3.4 Gross findings

Macroscopically, the osteoid osteoma looks like a small, round to oval and red gritty or granular lesion measuring less than 2 cm in diameter (23) (34). This benign tumor, that is often cortically based, is sharply demarcated and surrounded by a white sclerotic bone (22). The tumor can be soft, crumbly to solid sclerotic, and the middle of the nidus can seem to be more sclerotic than its boundary (3).

1.3.5 Histology

Microscopically, the tumor is sharp demarcated and consists of anastomosing thickened trabeculae composed of cancellous bone (3) that are surrounded by plump, metabolically active osteoblasts (23). Commonly, scattered osteoclast-like multinucleated giant cells can be found (3). Between, the intervening fibrous stroma is filled with prominent vascular network. Both osteoblasts and stromal cells do not show significant nuclear atypia or high mitotic activity. (6).

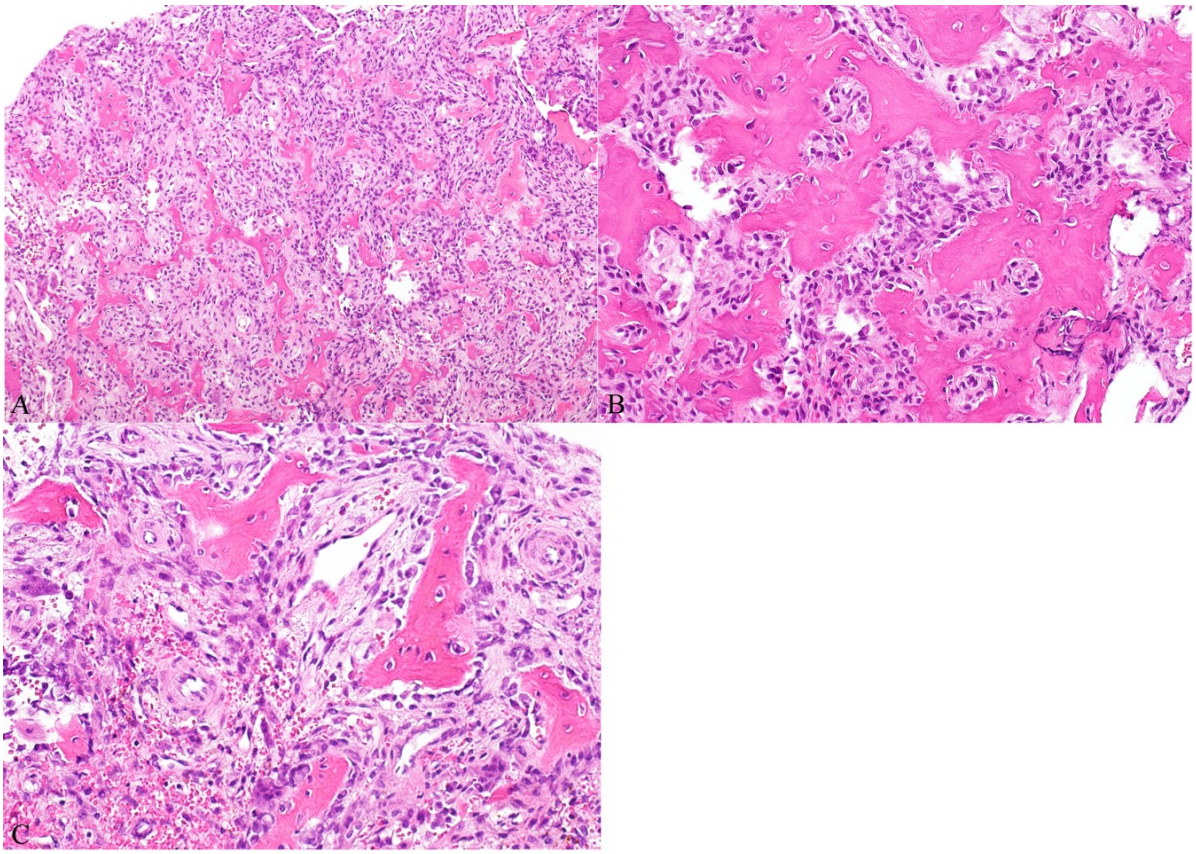

Figure 7: Example for OO showing trabeculae of woven bone, filled by osteoblasts and with vascular connective tissue stroma (A). (Hematoxylin-eosin, objective x10) Trabeculae of woven bone, with varying mineralization (B) (Hematoxylin-eosin, objective x20), Trabeculae with osteoblastic rims, Scattered giant cells in vascular stroma (C). (Hematoxylin-eosin, objective x20)

1.3.6 Differential diagnosis

The main differential diagnoses of an OO include osteoblastoma, osteosarcoma, osteomyelitis (e.g. Brodie abscess), bone island and stress fracture (3) and intracortical hemangioma (35). For the correct diagnosis, clinical history and radiologic imaging are significant. Furthermore, the radiological differential diagnoses also include cortical desmoid and osteochondroma.

1.3.6.1 Osteoblastoma

Osteoblastoma is rare and represents 1% of primary bone tumors. It occurs in men 2 times more often than in women and it affects young adults between second to fourth decades of life. It originates frequently in the posterior elements of the spine, sacrum and the metadiaphyseal region of long bones, especially the femur and proximal tibia (34). Typically, osteoblastoma may be locally aggressive and cause chronic pain with minimal response to NSAIDs, unlike OO.

Osteoblastoma and the OO are histological remarkably similar. The main distinctive feature of osteoblastoma is the considerable growth potential, with a nidus larger than 2 cm in diameter (34). Additionally, the lesion has a wide range of radiographic patterns, predominantly lytic expansive with a rim of reactive sclerosis and periostitis, possible soft tissue component and in rare cases associated aneurysmal bone cyst-like lesion (36). Histologically, osteoblastoma has less organized pattern of osteoid and reticular bone distribution (23).

Depending on the size and location, osteoblastoma is therapeutically treated by an aggressive curettage or en- bloc resection (34).

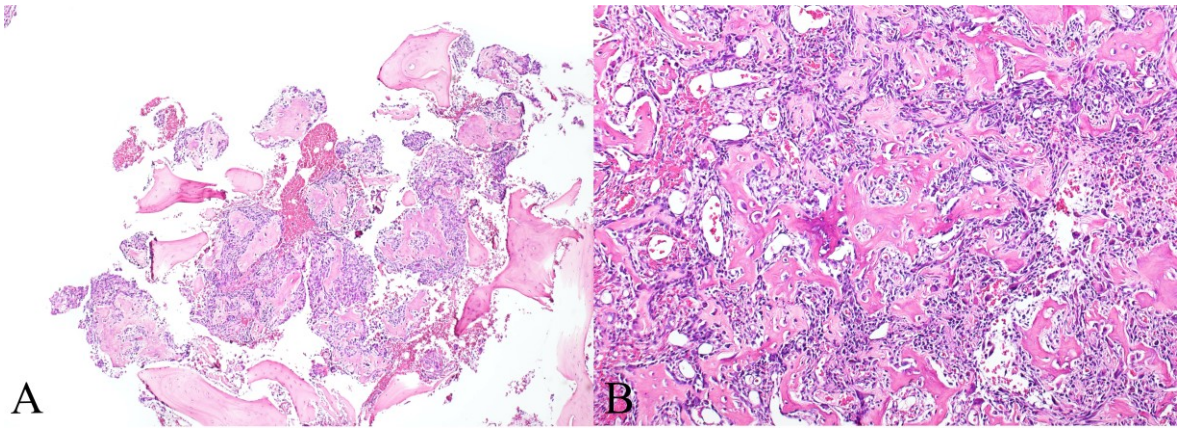

Figure 8: Bone lesion with a marginal sclerotic edge (A). (Hematoxylin-eosin, objective x4) A single layer of osteoblasts which are lining osseous trabeculae, Scattered multinucleated giant cells of osteoclast type, Regions of with extravasated erythrocytes (B). (Hematoxylin-eosin, objective x10)

1.3.6.2 Osteosarcoma

The most common primary malignant bone tumor is the conventional osteosarcoma. The tumor is highly malignant, and its neoplastic cells produce osteoid, with or without cartilaginous or fibroblastic components. Osteosarcoma arises in the intramedullary cavity or on the bone surface. Various subtypes of different histopathological phenotypes are described, having different grades, metastatic potential, and behavior.

The osteosarcoma occurs in men more common than in women at a ratio of 3:2 and the age of distribution has a first peak in children between 10 -14 years and a second peak in the third decade of life (34).

It can affect all bones of the appendicular skeleton but usually it originates in the metaphysis of long bones like the distal femur, proximal tibia, and proximal humerus.

Clinically, the conventional osteosarcoma presents as a rapidly destructive growing mass that causes profound pain. If located near joints, the tumor can reduce the range of motion.

According to the location, size, grade, and stage of the tumor the treatment is adapted to the age of the patient and includes wide resection of the primary tumor with or without radiation and/or adjuvant/neoadjuvant therapy and removal of metastases.

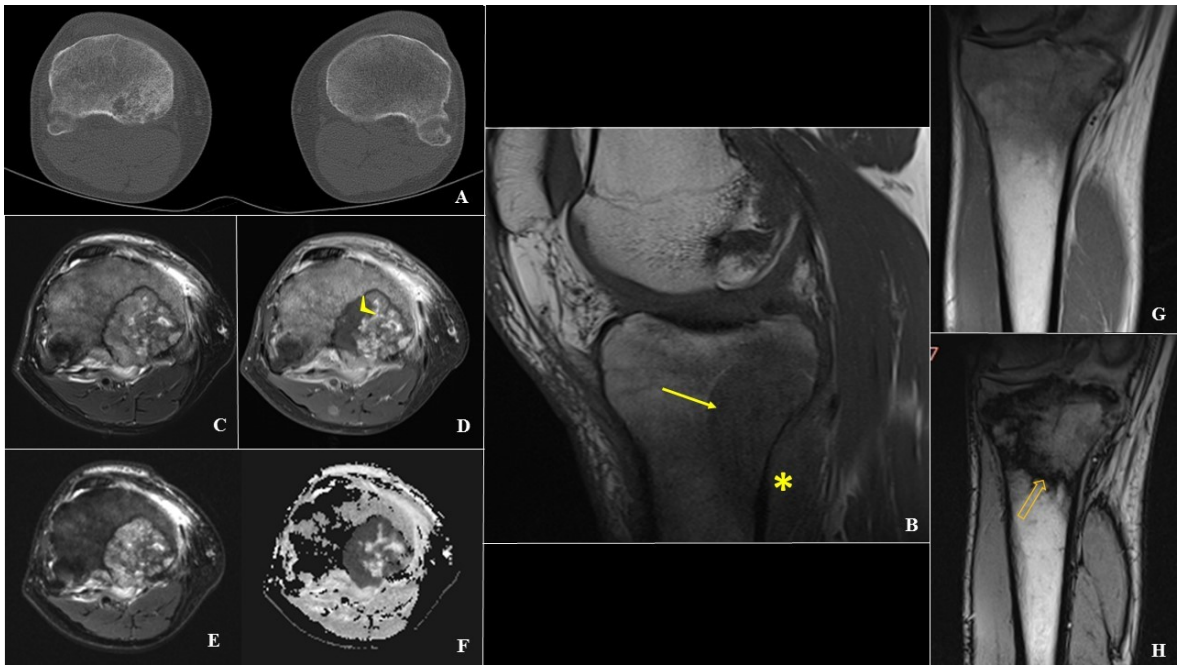

Figure 9: Classical osteosarcoma of the proximal tibial metaphysis in a 47-year-old male patient. A) Axial CT of the lower extremities in bone window show osteodestructive lesion in the medial proximal tibial metaphysis (yellow circle) B) Intraosseal (white arrow) and extraosseous (yellow star) extension of the tumor on sagittal T1-weighted sequence. C) Heterogenous signal intensity on the T2w-sequences; high-intensity areas correspond to hypovascularized or cystic areas. D) Heterogenous enhancement of the tumor on post gadolinium T1-weighted sequence with hypovascularized tumor tissue centrally. Diffusion restriction of the osteosarcoma on DWI- and ADC-map. (E, F) Chemical shift imaging - sharp delineation of the tumor and surrounding normal bone marrow with „India-ink artifact" on opposed phase (yellow arrow) (G, H)

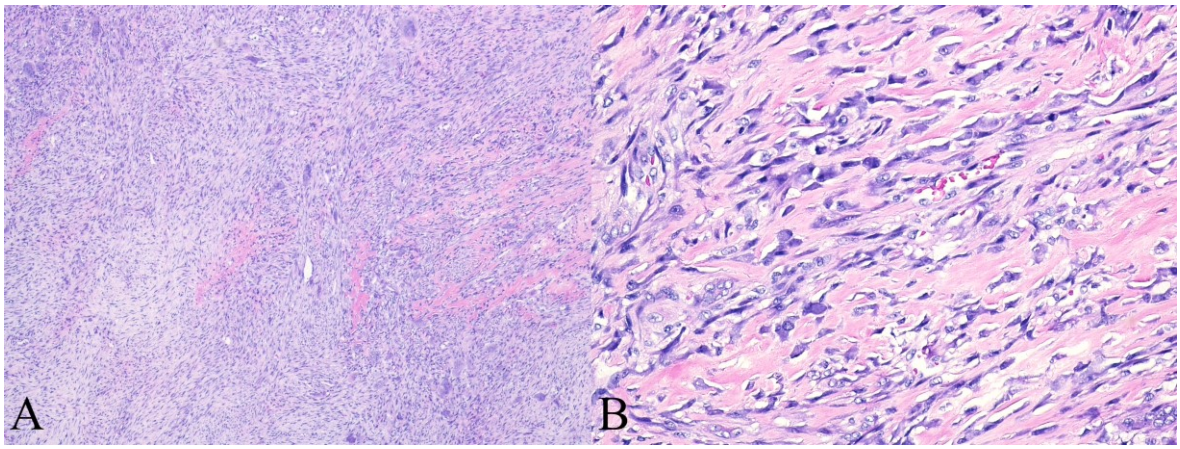

Figure 10: Osteosarcoma with permeative growth (A). (Hematoxylin-eosin, objective x4), Multiple neoplastic cells with pleomorphic, hyperchromatic nuclei, areas of filigree disorganized woven bone (B). (Hematoxylin-eosin, objective x20)

1.3.6.3 Inflammatory conditions

OO located in small bones of the hands and feet can mimic radiographically and clinically certain inflammatory conditions, such as chronic and subacute osteomyelitis (3).

Similarly as OO, these inflammatory conditions show increased radionuclide uptake on radionuclide bone scans which can prolongate the right and fast diagnosis of an OO(29). Three-phase bone scintigraphy helps differentiate these two entities showing typical increased vascularity in flow and blood pool phase and focal increased activity accumulation in the late phase which corresponds to nidus(37). On the other hand, the Brodie abscess is characterized with central area of reduced uptake representing an avascular area of purulent material (38).

A necrotic bone sequester is characteristic of long-standing osteomyelitis. On CR and CT it is possible to depict a lucent lesion with a central calcification representing a piece of devitalized bone as a which can mimic a nidus of an OO (39).

1.3.6.4 Bone island

Bone island, also known as enostosis, is benign and slow-growing lesion located in the intramedullary cavity of long bones (29). CR and CT usually show <1 cm large, homogeneous radio dense lesion with radiating spicules due to growth along the bony trabeculae The lesion greater than 2 cm in maximal dimension is called giant bone island. (40). A low signal intensity of bone island on all MRI-sequences is compatible with compact bone. Histologically, it is composed of mature compact lamellar and/or cancellous bone and lacks the perilesional sclerosis (3). The absence of pain or other clinical symptoms, in combination with a negative scintigraphy, helps to differentiate a bone island from an osteoblastic metastasis (23) (41).

1.3.6.5 Stress fracture

On imaging it is sometimes difficult to distinguish the endosteal reparative callus after stress fracture from reactive changes caused by OO. The clinical presentation is nevertheless different. In case of stress fractures, the patients present with worsening pain and a history of minimal or no trauma. When the lower limb is affected, there is often a history of recent increase or significant alteration in the physical activity. On the contrary, the patients with OO present with nocturnal pain, relieved by salicylates. (42). We can conclude that it is of outmost importance to visualize the nidus and collect patient data in detail.

1.3.7 Treatment

The treatment can be adjusted depending on the symptoms and location. Diverse types of treatment are currently available.

Patients with endurable symptoms are treated with NSAIDs to relieve pain and alleviate other symptoms. They can be followed-up with regular radiographs every four to six month (33).

The mechanism of NSAID treatment relies on the inhibition of the cyclooxygenase (COX), an enzyme which is relevant for the biosynthesis of prostaglandins (43). As COX occurs throughout the body , the range of side effects is wide including gastrointestinal bleeding, liver dysfunction, nephrotoxicity and cardiovascular complications (44).

For patients that suffer from intolerable pain or limp under NSAIDs- treatment, a more aggressive treatment is usually necessary, including surgical en-bloc resection or curettage and minimal invasive percutaneous radiofrequency ablation (RFA) (34).

1.3.7.1 Surgical resection

Surgical resection of osteoid osteoma is limited by the dissection size and the common need for cortical bone matrix transfer and internal fixation. Complications of surgical resection range at 9–28%. In addition, post resection pain persists in 7–20% due to osteomas recurrence. Alternative traditional surgical techniques for OO treatment include marginal resection of the entire nidus – En – block resection, curettage or high-speed burr techniques (45).

The en-bloc resection is preferred treatment option to remove the nidus and adjacent bone tissue (27). Despite high success rate of 88% to 100% (46), the method has several disadvantages, mainly regarding the identification of the location of tumor and resection margin, potentially leading to bone weakening and increased risk of insufficiency fracture (27).

Curettage can be used in anatomic sites where other treatments cannot be performed. Nevertheless, there is a high risk of incomplete nidus removal with a recurrence rate of up to 17% (29) (3).

1.3.7.2 Radiofrequency ablation

CT-guided percutaneous RFA is a simple, minimally invasive, safe, and highly effective technique for treating OO, with reported primary success rates of 83%–94% and secondary success rates of 89%–100%. Therefore, it is regarded as the modality of choice in most cases. Preinterventional diagnostic imaging (including CT and MRI) and proper localization of the lesion are of utmost importance for RFA-planning. Open surgery should be reserved for cases of persistent diagnostic uncertainty or spinal lesions, which do not respond to medical treatment and/or cannot be heated safely because of close relation to vital soft tissue structures (47). In comparison to surgical treatment methods, the RFA is cost-effective with shorter in-hospital stay.(27) (46).

Commonly, the RFA is performed under general anesthesia with prophylactic intravenous application of antibiotics. After patient positioning and fixation, skin preparation and local periosteal anesthesia, contiguous CT scans using stereotactic navigation system (in our institution CAS-One, CAScination) is obtained for precise preprocedural localization of the nidus. Osseous access to the nidus is established under the CT-guidance with the use of either a biopsy-needle or a coaxial drill system, depending on the localization of the nidus relative to the bone surface and the amount of adjacent bone sclerosis.

Biopsy of the lesions is usually performed in case of inconclusive imaging findings and to exclude malignancy. Following biopsy, the needle is exchanged for the active tip monopolar radiofrequency electrode with different lengths (in our institution Rita StarBurst, AngioDynamics, 14 G) and CT imaging is done to confirm the placement of the tip within the nidus.

The temperature of thermocoagulation produced by the electrode is of utmost importance for successful ablation of the nidus, whereas low temperature will not result in coagulation of the tumor. On the other hand, too high temperature leads to evaporation of the adjacent tissue, thus preventing the correct heat dispersion through the lesion (46). Keeping this in mind, the tip of the electrode is heated to 90°C for a period of 4-6 minutes (6). Postprocedural CT is performed to confirm the lack of soft tissue swelling and hematoma.

Determined by institutional preference, after the procedure and depending on the lesion localization, partial weight-bearing for certain time (2-3 weeks) is advised. In the case of post-interventional burns, antibiotic therapy is advised. Follow-up is usually performed with MRI or CT (46).

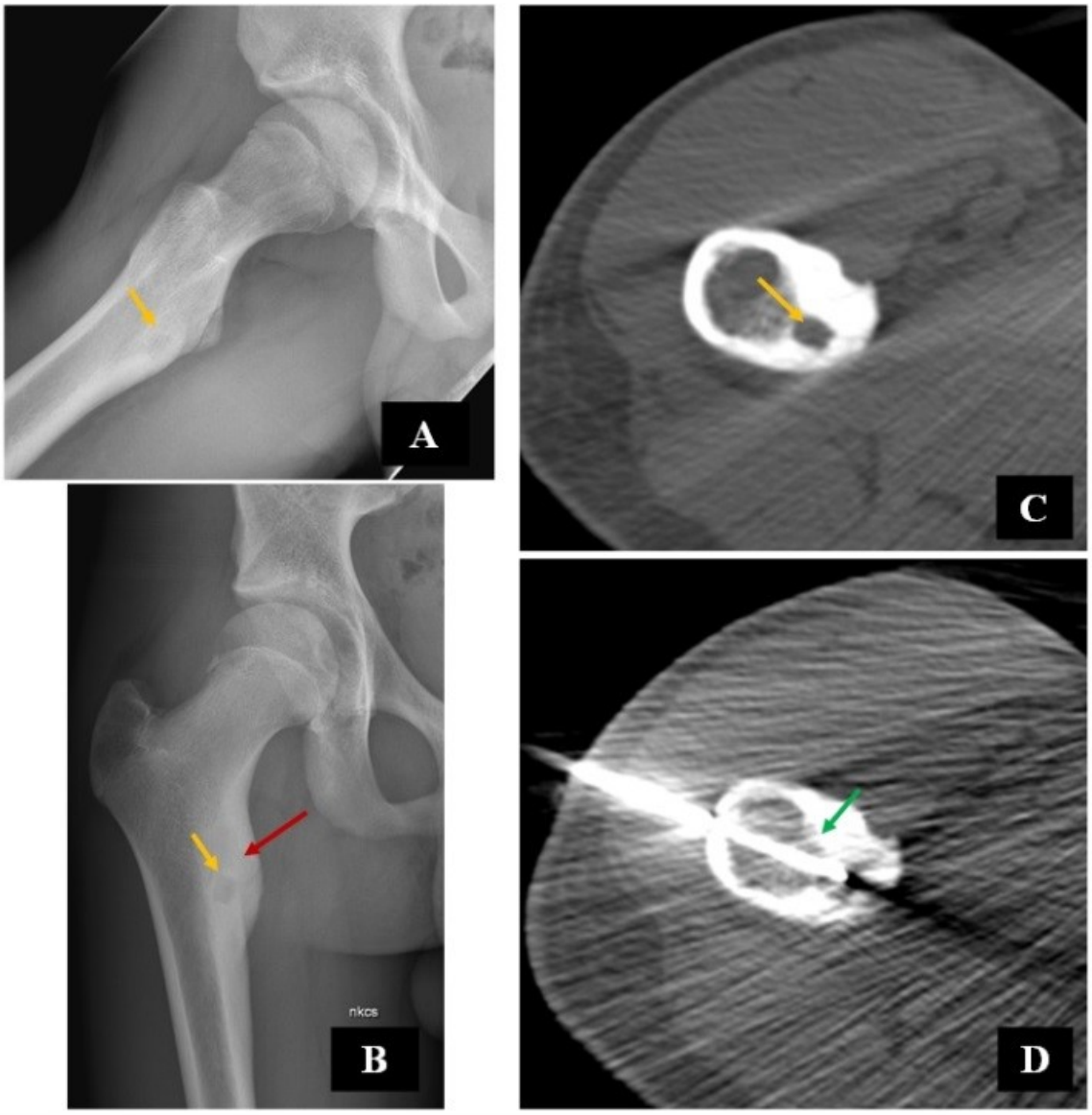

Figure 11: A 12-year-old male patient with osteoid osteoma treated with radiofrequency ablation. Radiographs of the right hip in 2 projections depict the cortical thickening of the minor trochanter with 7 mm central lucency (yellow sclerosis) and surrounding reactive bone sclerosis (red arrow), typical imaging findings for osteoid osteoma. Corresponding, preprocedural axial CT image of the proximal femur (C). Intraprocedural axial CT image with electrode tip placed in the center of nidus (green arrow) (D).

1.3.8 Prognosis

OO have excellent prognosis after RFA or total surgical excision (23) with complete symptom relief (33). The local recurrence can occur after partial excision or ablation of the lesion (48).

2 Material and methods

A retrospective data collection and literature search, including PubMed bibliographic database and specialized pathology books, was performed.
A retrospective single center study was performed to analyze epidemiological, clinical, and radiological findings of patients with OO treated in our institution. In addition, the type of treatment and the success /complication rate between surgical resection and CT- guided percutaneous RFA were analyzed.
This retrospective study was approved by the Ethic Committee of the Medical University of Graz (EK-Nummer 33-265 ex 20/21).

2.1 Study population

The study population of this retrospective analysis included 122 patients with OO, diagnosed at the D&R Institute of Pathology, Department of Radiology, and Department of Orthopedics and Trauma, Medical University of Graz, in a period from January 2005 to September 2019.
Patients of all genders were selected from the electronic register of the Department of Orthopedics and Trauma. Inclusion criteria were radiologically and/or histologically confirmed diagnosis of OO in the planned time interval with adequate clinical data.
Imaging findings (CT and/or MRI) of all patients were re-evaluated.

2.2 Analytical data

The data was collected from the patient files from “openMedocs" and anonymized.
The analysis included following clinical data: age, gender, symptoms (and duration), date of CT examination, date of MRI examination, differential diagnosis on CT/MR, tumor location, tumor size, date of surgery, histological findings (in cases where material was available), date of RFA, date of local recurrence, date of surgery or RFA for local recurrence, type of postoperative or postinterventional complication, type of symptoms.

2.3 Statistical analysis

Data were analyzed using Microsoft Excel for Mac (Microsoft, Redmond, Washington, USA), and IBM SPSS Statistics 25 (IBM, Chicago, Illinois, USA). The regression model was used to describe a trend in the reduction of incidence rates. Two-sample Wilcoxon rank-sum (Mann–Whitney) test was conducted to describe differences between the groups (spinal vs extraspinal). P-values < 0.05 were considered statistically significant.

3 Results

The study cohort included 122 patients; 43 (35.2%) were females and 79 (64.8%) males. The median age was 21.2 years with an age range from 2 to 63 years (Table 3). The clinical and radiological findings are summarized in Table 8.

Table 2: Age distribution of patients with osteoid osteoma

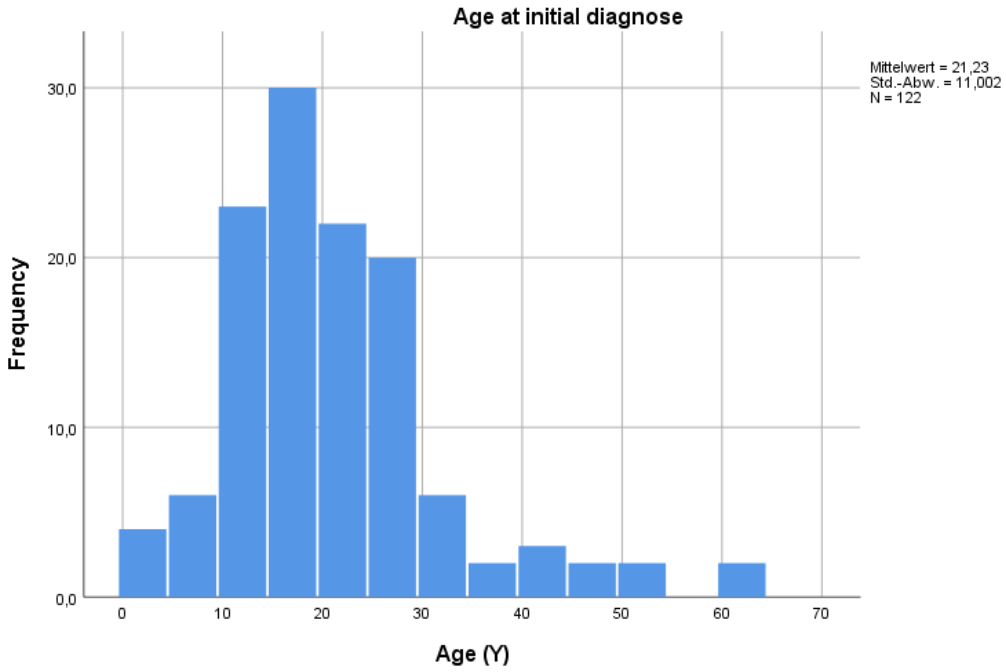

Table 3: Descriptive statistics of age, symptom duration and lesion size

	N	Minimum	Maximum	Mean	Standard deviation
Age (J)	122	2	63	21,23	11,002
Symptom duration (months)	121	,5	120,0	13,252	17,4350
Lesion size (mm)	122	2	25	8,65	4,987

CT was performed in 108 patients, and MRI was performed in 106 patients. Of 108 CTs performed, in 90 cases (83,3%) lesions were confirmed, in 18 cases no lesion could be verified by CT (Table 4). Out of these 18 cases, in 3 a lesion could be verified by MRI.
In 14 patients without CT imaging, a lesion was confirmed by MRI in 12 cases. In the last two patients, in one case no lesion was found using MRI and in one case, no MRI was performed

Table 4: Cross tab of performed/not performed CT & CT confirmed/not confirmed lesion

		CT		
		lesion not confirmed	lesion confirmed	Total
CT not performed	14	0	0	14
CT performed	0	18	90	108
Total	**14**	**18**	**90**	**122**

Of 106 MRIs performed, in 69 cases (65,1%) lesions were confirmed, and in 37 cases no lesion could be verified by MRI (Table 5). Out of these 37 cases, in 21 a lesion could be verified by CT. In 16 patients without MRI imaging, a lesion was confirmed by CT in 15 cases. In one patient, no CT was performed.
In the case of 15 patients neither by CT nor by MRI, a lesion could be confirmed.

Table 5:Cross tab of performed/not performed MRI & MRI confirmed/not confirmed lesion

		MRI		
		lesion not confirmed	lesion confirmed	Total
MRI not performed	16	0	0	16
MRI performed	0	37	69	106
Total	**16**	**37**	**69**	**122**

The lesions were most frequently located in the femur (n=39; 32%), the tibia (n=37; 30,3%), the humerus (n=9; 7,4%), and the radius (n=4; 3,3%). The rest of the lesions (n=34, 27,9%) were in fibula, spine, feet, sacrum, hands, scapula, patella, ulna, and acetabulum (Table 6).

Table 6: Body location of the lesions

Location	Number	Percentage (%)
Acetabulum	1	0,8
Acromion	1	0,8
Carpus	1	0,8
Femur	39	32,0
Fibula	3	2,5
Finger	2	1,6
Humerus	9	7,4
Lumbar spine	3	2,5
MC	2	1,6
MCP-joint	2	1,6
Patella	2	1,6
Radius	4	3,3
Sacrum	3	2,5
Scapula	1	0,8
Talus	3	2,5
Tarsus	1	0,8
Thoracic spine	2	1,6
Tibia	37	30,3
Toe	2	1,6
Ulna	2	1,6
Unknown	2	1,6
Total	**122**	**100,0**

Lesions were located cortically in 79.5% of the cases. Further locations of lesions were subperiosteal in 6.6%, intracapsular and medullary in 5.7%. In one patient the lesions were multifocal.

The mean diameter of the nidus was 8.65 ± 5,0 mm (range 2 – 25 mm). A delay in the diagnosis was 13.3 ± 17.4 months (Table 3).

A total of 118 patients underwent treatment at our institution: 71 (60.2%) were treated with RFA and 42 (35.6%) underwent surgery. A small number of 5 (4.2%) patients underwent both treatments, RFA and surgery. 4 patients received conservative treatment. (Table 8).
Out of 71 patients treated with RFA, relapses occurred in 7 (9.9%) cases. This corresponds to a treatment success rate of 90.1%, respectively. In 42 patients who underwent surgery, recurrences were observed in 8 (19.1%) cases. In this form of therapy, the treatment success rate was 81.0%, respectively. The 5 patients who were treated with both therapy methods recorded a relapse in 1 (20%) case. That means a treatment success rate of 80%.

Table 7:Total number of complications during and after treatment

	Number	Percentage (%)
N	108	88,5
Y	14	11,5
Total	**122**	**100,0**

In 108/122 patients, no interventional or post-operative complications could be observed. In 14 cases, complications occurred during the procedure or after the intervention (Table 7). The outcome of all patients with listed complications is summarized in Table 8.
In detail, in 11 cases complications occurred in patients undergoing RFA treatment (complication rate of 15.5%). In the additional three cases, complications developed during/after surgery (a complication rate of 7.1%).

Table 8: Summarized outcome of all patients with listed complications.

		RFA	OP	RFA&OP	conservative treatment	Total
Number of executed therapies in our institution						
	Treatment	71	42	5	4	122
Types of complications during and after treatment						
	Prolonged pain	2	1	0	_	3
	Anesthetic accident	2	0	0	_	2
	Thermal skin damage	3	0	0	_	3
	Local complication*	2	2	0	_	4
	Movement disorder	1	0	0	_	1
	Technical defect°	_	_	1	_	1
Total	(complications rate)	10(16,1%)	3(7,1%)	1(20%)	_	14
*(hypertrophic scar, soft tissue inflammation and fistula, slight numbness in the right groin, insufficiency fracture) °(Needle breakage)						
		RFA	OP	RFA&OP	conservative treatment	Total
Treatment outcome at follow-up examination after one week						
	Persistent symptoms*	5(7%)	2(4,75%)	0	3(75%)	10
	Scar pain	1(1,4%)	2(4,75%)	0	0	3
	Asymptomatc	65(91,6%)	38(90,5%)	5(100%)	1(25%)	109
Total		71	42	5	4	122
*(declining pain, hypesthesia, pain after overload, swelling without pain, post-RFA Synovitis with residual pain)						

After one week, all treated patients had a control examination. In 109 of 122 patients (89,3%), pain could be relieved after RFA (91,6%), surgery (90,5%), RFA & surgery (100%) or conservative treatment (25%). Another 4 patients reported declining pain after treatment with RFA. (Table 8) Further 6 patients reported still suffering from consequences of the intervention one week ago. After surgical treatment, 2 patients had scar pain, 1 had swelling without pain and 1 patient had pain after overload. With the minimally invasive RFA,1 patient had scar pain and 1 patient suffered from post-RFA synovitis with residual pain. 3 Patients treated conservatively suffered from declining pain, hypesthesia and pain after overload at follow-up examination. At the follow-up examination, all 14 patients who experienced complications during/after intervention with RFA, OP or RFA & OP were asymptomatic.

4 Discussion

In this study we describe 122 patients with OO treated in a 15-year period. We showed that this benign tumor is more commonly found in men as they were nearly two times more often affected than female patients (male: female=1,8:1). Our retrospective analysis of patient data showed that OO manifests in 80% between 5 and 30 years of age. Nevertheless, outliers were observed in our study population: the youngest patient was two years old, and the oldest patient was 63 years at the time of diagnosis. The epidemiological and clinical data in our study correlate with the data described in the literature (3). The OO was most frequently located in the tubular bones of the lower extremity, most commonly in femur and tibia, followed by the long tubular bones of the upper extremity, arising in humerus and radius. About half of the femoral lesions affected the trochanteric region or the femoral neck. In the tibia, the diaphysis was most affected. Humerus lesions were located proximally, whereas tumors of the radius arose more frequently in the distal part. The remaining lesions involved smaller bones of the lower and upper extremities, as well as the spine (lumbar spine and sacrum being the most affected). Localization of the tumors was usually in the cortex, rarely subperiosteal, intracapsular and medullary.

The mean diameter of the nidus was approximately 9 mm (the smallest nidus measuring 2 mm and the largest with a diameter of 25 mm). In the latter case the size is atypical for an OO and the histology was inconclusive (it was not possible to differentiate between OO and osteoblastoma). However, the clinical symptoms were in favor of OO.

In imaging analysis, CT is superior to MRI as it demonstrates the nidus in OO. High resolution thin-section axial and longitudinal multiplanar reformatted CT images are obtained with a bone algorithm and viewed with bone window settings for the detection of the nidus. In addition, this technic should help exclude other differential diagnosis including osteoblastoma, osteomyelitis, stress fracture, arthritis, and enostosis. To depict the rapid early arterial enhancement of the nidus (as the nidus is hypervascular), dynamic contrast-

enhanced CT can be used for, in case of an atypical clinical presentation, exclusion of avascular changes like Brodie abscess and bone cyst (35, 45). At CT, the nidus is well defined and round or oval with low attenuation. An area of high attenuation may be seen centrally, a finding that represents mineralized osteoid. In addition, CT can be useful in identifying the origin of a tumor, and in assessing the relationship of the tumor to the medulla. However, a standard CT cannot demonstrate soft tissue or bone marrow edema. MRI can depict the nidus and accompanying sclerosis - the nidus has low to intermediate signal intensity on T1-weighted images and variable signal intensity on T2-weighted images, depending on the amount of mineralization present in the center of the nidus. In selected cases, in juxta- articular located tumors, reactive changes (such as cortical thickening and medullary sclerosis) are lacking, and a predominant synovitis may be present, which is preferentially appreciated using MRI (49-51). Although the MRI is more sensitive than CT scan for detection of reactive changes in the soft tissue and surrounding bone edema, these can sometimes obscure the lesion itself and mimic an infection or a malignant tumor (33, 49, 52). Further on, joint effusion may also be appreciated. Nevertheless, due to a spectrum of radiomorphological presentations, in most cases, the combination of CT and MRI can lead to the correct diagnosis. In our study population (122 patients), 108 CTs and 106 MRIs were performed. The data analysis showed that in 90/108 cases (83.3%) a lesion was confirmed by CT. Of the 106 MRIs performed, a lesion was confirmed in 69 cases (65.1%). This shows a higher accuracy of CT in diagnosing OO than that of MRI. Furthermore, in 21/37 (not confirmed by MRI) cases, a lesion could be verified by CT. In comparison, only 3/18 with an MRI. After CR, the decision about advanced imaging is usually made individually for each patient to confirm the OO. If CR and CT are not sufficient to confirm the OO, an additional MRI is performed in most cases to establish the diagnosis.

Percutaneous CT-guided RFA of OO is a minimally invasive alternative treatment to the surgical and medical management of OO. Preinterventional diagnostic imaging with CT and /or MRI and localization of the lesion are very important for RFA-planning. In our study, we showed that the RFA is a solid, and efficient therapy for OO with a treatment success rate of about 90%. Out of all with RFA treated patients, only 7 (9.9%) showed a recurrence

or a rest tumor. This is similar to Bourgaults study on CT guided RFA of osteoid osteoma with a reported recurrence rate of 10.4% (53).

At the follow-up examination 7 days after RFA, 65 patients reported pain relief. This corresponds to a clinical success rate of over 91% with a pain disappearance straight after the RFA. Four more patients reported declining pain after RFA procedure. Our clinical success rate is comparable with the data analysis of 27 articles of Lanza et al., consisting of 1,772 patients with OO treated with minimal-invasive RFA and a success rate of 90-100% (54). Furthermore, therapy costs with RFA are lower and are approximately 25% less expensive than an open procedure (55). In addition, the length of hospital stay for RFA is significantly shorter than for a surgical procedure. This circumstance is characterized positively for the patients since the treatment is less time-consuming. This in turn means higher patient acceptance of the therapy (56).

At the control examination one week after surgery, 38 patients reported pain relief. This complies with a clinical success rate of 90,5%. Smolle et al. recorded a comparable outcome with 90% of symptomatically pain relief after open surgery (57). In our study population, surgical treatment of the lesions resulted in postoperative recurrence in 19% of cases. This suggests that the treatment success rate of 81% is almost 10% lower than with minimally invasive RFA. Göksel et al. reported recurrence rate of 18,1% for curettage, very similar to our study (58). Rosenthal described a lower (9%) recurrence treated with open procedures (55). These results shows that open surgery should be reserved for cases of persistent diagnostic uncertainty or spinal lesions, which do not respond to medical treatment and/ or cannot be heated safely because of the close relation to vital soft tissue structures (47).
An unexpected but interesting outcome in our data analysis is the fact that the complication rate, during and after treatment, for the minimally invasive RFA variant is twice as high as for the surgical method. In two cases of preparation for RFA intervention, unexpected complications during anesthesia occurred, including allergic reaction to the anesthetic and difficult intubation due to a swollen epiglottis. The general reported RFA complication rate

was about 3%, within skin burns as most common one followed by infections (59). For surgical complications, Sluga et al., reported postoperative fractures in 3% (60).
At the follow-up examination one week after treatment, all patients were asymptomatic.

Our study has some limitations: First the retrospective study only refers to monocentric collected data from our Medical University of Graz and thus the significance is not valid across countries regionally. Second, the success of OO treatment also depends on the technical skills of the treating physicians. Another limitational factor in our study is the short follow-up of only one week.

4.1 Conclusion

In conclusion, our study shows that OO is predominantly found in male patients, is frequently arising in the lower extremities, and is usually located cortically. Concordant to the literature, a significant delay in diagnosis of OO was found. RFA is a simple, minimally invasive, safe, and highly effective technique for treating OO with high success rates. Compared to surgical treatment, RFA is a reliable and efficient treatment option for OO.

References

1. Anderhuber F, Pera F, Streicher J. Waldeyer Anatomie des Menschen. 19 ed. Berlin: De Gruyter; 2012: p.94.
2. Grabowski P. Physiology of bone. Endocr Dev. 2009;16:32-48.
3. Dorfman HD, Czerniak B. Dorfman and Czerniak's Bone Tumors. 2 ed. Philadelphia Elsevier; 2015: p. 3-162.
4. Clarke B. Normal bone anatomy and physiology. Clin J Am Soc Nephrol. 2008;3 Suppl 3(Suppl 3):S131-9.
5. Lüllmann-Rauch R. Histologie. 5 ed. Stuttgart: Georg Thieme Verlag; 2015: p. 131-312.
6. Vigorita VJ. Orthopadic Pathology. 2 ed. Philadelphia: Wolters Kluwer Health; 2008: p. 6-343.
7. Parfitt AM. Misconceptions (2): turnover is always higher in cancellous than in cortical bone. Bone. 2002;30(6):807-9.
8. Akkus O, Polyakova-Akkus A, Adar F, Schaffler MB. Aging of microstructural compartments in human compact bone. J Bone Miner Res. 2003;18(6):1012-9.
9. Ott SM. Cortical or Trabecular Bone: What's the Difference? Am J Nephrol. 2018;47(6):373-5.
10. Platzer W. 1 Bewegungsapperat 11 ed. Stuttgart: Georg Thieme Verlag; 2013: p. 166
11. Travlos GS. Normal structure, function, and histology of the bone marrow. Toxicol Pathol. 2006;34(5):548-65.
12. Mohamed AM. An overview of bone cells and their regulating factors of differentiation. Malays J Med Sci. 2008;15(1):4-12.
13. Xiong J, Onal M, Jilka RL, Weinstein RS, Manolagas SC, O'Brien CA. Matrix-embedded cells control osteoclast formation. Nat Med. 2011;17(10):1235-41.
14. Florencio-Silva R, Sasso GRdS, Sasso-Cerri E, Simões MJ, Cerri PS. Biology of Bone Tissue: Structure, Function, and Factors That Influence Bone Cells. BioMed Research International. 2015;2015:421746.
15. Manolagas SC. Birth and death of bone cells: basic regulatory mechanisms and implications for the pathogenesis and treatment of osteoporosis. Endocr Rev. 2000;21(2):115-37.
16. Jilka RL, Weinstein RS, Bellido T, Parfitt AM, Manolagas SC. Osteoblast Programmed Cell Death (Apoptosis): Modulation by Growth Factors and Cytokines. Journal of Bone and Mineral Research. 1998;13(5):793-802.
17. Chen X, Wang Z, Duan N, Zhu G, Schwarz EM, Xie C. Osteoblast-osteoclast interactions. Connect Tissue Res. 2018;59(2):99-107.
18. Teitelbaum SL, Ross FP. Genetic regulation of osteoclast development and function. Nat Rev Genet. 2003;4(8):638-49.
19. Insogna KL, Sahni M, Grey AB, Tanaka S, Horne WC, Neff L, et al. Colony-stimulating factor-1 induces cytoskeletal reorganization and c-src-dependent tyrosine

phosphorylation of selected cellular proteins in rodent osteoclasts. J Clin Invest. 1997;100(10):2476-85.
20. Board WCoTE. Soft Tissue and Bone Tumours. 5 ed: International Agency for Research on Cancer; 2020: p. 862,867.
21. Böcker W, Denk H, Heitz PU, Moch H, Höfler G, Kreipe H. Lehrbuch Pathologie. 5 ed. München: Elsevier GmbH; 2012: p. 342-867.
22. WHO Classification of Tumours, Editorial Board. Soft Tissue and Bone Tumours. 5 ed: International Agency for Research on Cancer; 2020: p. 35-395.
23. Greenspan A., Borys D. Radiology and Pathology Correlation of Bone Tumors. Philadelphia: Wolters Kluwers; 2015: p. 35-40.
24. Parmeggiani A, Martella C, Ceccarelli L, Miceli M, Spinnato P, Facchini G. Osteoid osteoma: which is the best mininvasive treatment option? Eur J Orthop Surg Traumatol. 2021;31(8):1611-24.
25. Orth P, Kohn D. [Diagnostics and treatment of osteoid osteoma]. Orthopade. 2017;46(6):510-21.
26. Wold LE, Pritchard DJ, Bergert J, Wilson DM. Prostaglandin synthesis by osteoid osteoma and osteoblastoma. Mod Pathol. 1988;1(2):129-31.
27. Dookie AL, Joseph RM. Osteoid Osteoma. StatPearls. Treasure Island (FL): StatPearls Publishing
Copyright © 2020, StatPearls Publishing LLC.; 2020.
28. May CJ, Bixby SD, Anderson ME, Kim YJ, Yen Y-M, Millis MB, et al. Osteoid Osteoma About the Hip in Children and Adolescents. JBJS. 2019;101(6):486-93.
29. Deyrup AT, Siegal GP. Practical Orthopedic Pathology
A Diagnostic Approach. Philadelphia: Elsevier; 2016: p. 67-73.
30. Carneiro BC, Da Cruz IAN, Ormond Filho AG, Silva IP, Guimarães JB, Silva FD, et al. Osteoid osteoma: the great mimicker. Insights Imaging. 2021;12(1):32.
31. Hashemi J, Gharahdaghi M, Ansaripour E, Jedi F, Hashemi S. Radiological features of osteoid osteoma: pictorial review. Iran J Radiol. 2011;8(3):182-9.
32. Edeiken J, Hodes PJ. Roentgen diagnosis of diseases of bone. Roentgen diagnosis of diseases of bone; 1973.
33. Tis JE. Nonmalignant bone lesions in children and adolescents. In: Post T, editor. UpToDate, Waltham, MA. (Accessed on March 26, 2020): UpToDate.
34. Zhang Y, Rosenberg AE. Bone-Forming Tumors. Surg Pathol Clin. 2017;10(3):513-35.
35. Chai JW, Hong SH, Choi JY, Koh YH, Lee JW, Choi JA, et al. Radiologic diagnosis of osteoid osteoma: from simple to challenging findings. Radiographics. 2010;30(3):737-49.
36. Hu H, Wu J, Ren L, Sun X, Li F, Ye X. Destructive osteoblastoma with secondary aneurysmal bone cyst of cervical vertebra in an 11-year-old boy: case report. Int J Clin Exp Med. 2014;7(1):290-5.
37. Park JH, Pahk K, Kim S, Lee SH, Song SH, Choe JG. Radionuclide imaging in the diagnosis of osteoid osteoma. Oncol Lett. 2015;10(2):1131-4.
38. Bahk Y-W. Combined Scintigraphic and Radiographic Diagnosis of Bone and Joint Diseases. 5 ed. Heidelberg: Springer Verlag 2018.

39. Jennin F, Bousson V, Parlier C, Jomaah N, Khanine V, Laredo JD. Bony sequestrum: a radiologic review. Skeletal Radiol. 2011;40(8):963-75.
40. Nielsen GP, Rosenberg AE. Diagnostic pathology: bone: Elsevier Health Sciences; 2021.
41. Ulano A, Bredella MA, Burke P, Chebib I, Simeone FJ, Huang AJ, et al. Distinguishing Untreated Osteoblastic Metastases From Enostoses Using CT Attenuation Measurements. AJR Am J Roentgenol. 2016;207(2):362-8.
42. Mandell JC, Khurana B, Smith SE. Stress fractures of the foot and ankle, part 2: site-specific etiology, imaging, and treatment, and differential diagnosis. Skeletal Radiol. 2017;46(9):1165-86.
43. Bacchi S, Palumbo P, Sponta A, Coppolino MF. Clinical pharmacology of non-steroidal anti-inflammatory drugs: a review. Antiinflamm Antiallergy Agents Med Chem. 2012;11(1):52-64.
44. Graefe K-H, Lutz W, Bönisch H. Pharmakologie und Toxikologie. 2., vollständig überarbeitete Auflage ed. Stuttgart: Thieme; 2016.
45. Noordin S, Allana S, Hilal K, Nadeem N, Lakdawala R, Sadruddin A, et al. Osteoid osteoma: Contemporary management. Orthop Rev (Pavia). 2018;10(3):7496.
46. De Filippo M, Russo U, Papapietro VR, Ceccarelli F, Pogliacomi F, Vaienti E, et al. Radiofrequency ablation of osteoid osteoma. Acta Biomed. 2018;89(1-S):175-85.
47. Woertler K, Vestring T, Boettner F, Winkelmann W, Heindel W, Lindner N. Osteoid osteoma: CT-guided percutaneous radiofrequency ablation and follow-up in 47 patients. J Vasc Interv Radiol. 2001;12(6):717-22.
48. Shields DW, Sohrabi S, Crane EO, Nicholas C, Mahendra A. Radiofrequency ablation for osteoid osteoma - Recurrence rates and predictive factors. Surgeon. 2018;16(3):156-62.
49. Allen SD, Saifuddin A. Imaging of intra-articular osteoid osteoma. Clin Radiol. 2003;58(11):845-52.
50. Lalam R, Bloem JL, Noebauer-Huhmann IM, Wörtler K, Tagliafico A, Vanhoenacker F, et al. ESSR Consensus Document for Detection, Characterization, and Referral Pathway for Tumors and Tumorlike Lesions of Bone. Semin Musculoskelet Radiol. 2017;21(5):630-47.
51. Bhure U, Roos JE, Strobel K. Osteoid osteoma: multimodality imaging with focus on hybrid imaging. Eur J Nucl Med Mol Imaging. 2019;46(4):1019-36.
52. Torriani M, Rosenthal DI. Percutaneous radiofrequency treatment of osteoid osteoma. Pediatric Radiology. 2002;32(8):615-8.
53. Bourgault C, Vervoort T, Szymanski C, Chastanet P, Maynou C. Percutaneous CT-guided radiofrequency thermocoagulation in the treatment of osteoid osteoma: a 87 patient series. Orthop Traumatol Surg Res. 2014;100(3):323-7.
54. Lanza E, Thouvenin Y, Viala P, Sconfienza LM, Poretti D, Cornalba G, et al. Osteoid osteoma treated by percutaneous thermal ablation: when do we fail? A systematic review and guidelines for future reporting. Cardiovasc Intervent Radiol. 2014;37(6):1530-9.
55. Rosenthal DI, Hornicek FJ, Wolfe MW, Jennings LC, Gebhardt MC, Mankin HJ. Percutaneous radiofrequency coagulation of osteoid osteoma compared with operative treatment. J Bone Joint Surg Am. 1998;80(6):815-21.

56. Yu X, Wang B, Yang S, Han S, Jiang L, Liu X, et al. Percutaneous radiofrequency ablation versus open surgical resection for spinal osteoid osteoma. Spine J. 2019;19(3):509-15.
57. Smolle MA, Gilg MM, Machacek F, Smerdelj M, Tunn PU, Mavcic B, et al. Osteoid osteoma of the foot : Presentation, treatment and outcome of a multicentre cohort. Wien Klin Wochenschr. 2021.
58. Göksel F, Aycan A, Ermutlu C, Gölge UH, Sarısözen B. COMPARISON OF RADIOFREQUENCY ABLATION AND CURETTAGE IN OSTEOID OSTEOMA IN CHILDREN. Acta Ortop Bras. 2019;27(2):100-3.
59. Tordjman M, Perronne L, Madelin G, Mali RD, Burke C. CT-guided radiofrequency ablation for osteoid osteomas: a systematic review. Eur Radiol. 2020;30(11):5952-63.
60. Sluga M, Windhager R, Pfeiffer M, Dominkus M, Kotz R. Peripheral osteoid osteoma. Is there still a place for traditional surgery? J Bone Joint Surg Br. 2002;84(2):249-51.